CONFIDENTIAL

309

Copy
RM E56K29a

NACA RM E56K29a

NACA

# RESEARCH MEMORANDUM

## COMPARISON OF RESULTS OF EXPERIMENTAL AND THEORETICAL STUDIES OF BLADE-OUTLET BOUNDARY-LAYER CHARACTERISTICS OF STATOR BLADE FOR A HIGH SUBSONIC MACH NUMBER TURBINE

By Cavour H. Hauser and William J. Nusbaum

Lewis Flight Propulsion Laboratory
Cleveland, Ohio



CLASSIFIED DOCUMENT



NATIONAL ADVISORY COMMITTEE
FOR AERONAUTICS

WASHINGTON

February 15, 1957

CONFIDENTIAL

NATIONAL ADVISORY COMMITTEE FOR AERONAUTICS

RESEARCH MEMORANDUM

# COMPARISON OF RESULTS OF EXPERIMENTAL AND THEORETICAL STUDIES OF BLADE-OUTLET BOUNDARY-LAYER CHARACTERISTICS OF STATOR BLADE FOR A HIGH SUBSONIC MACH NUMBER TURBINE

By Cavour H. Hauser and William J. Nusbaum

## SUMMARY

Experimental boundary-layer-flow surveys for a stator blade are analyzed and compared with results obtained from a theoretical analysis. Results of surveys of the boundary-layer thickness at the blade mean radius in the plane of the blade trailing edge are compared with a theoretical calculation of the momentum thickness assuming a turbulent boundary layer. Also, the over-all total-pressure ratio across the stator calculated from the mean-radius boundary-layer surveys is compared with a value obtained from the over-all annular survey a short distance downstream of the blade row.

Although good agreement is obtained at low velocities, the measured values of boundary-layer momentum thickness from the mean-radius trailing-edge surveys are greater than the theoretical values at the higher exit velocities. This difference is probably due in part to inward radial flow of the low-momentum boundary-layer fluid near the outer portion of the blade.

The over-all total-pressure ratio calculated from the mean-radius trailing-edge surveys is somewhat less than that obtained from the annular surveys over a range of exit critical velocity ratio. Apparently, radial inward flow of the low-momentum fluid near the blade tip caused the loss measured at the mean radius to be greater than an average value for the whole blade passage.

## INTRODUCTION

In order to obtain a better understanding of the fundamental nature of the losses occurring in turbomachine blade rows, a research program is being carried out at the NACA Lewis laboratory in which the results of both theoretical and experimental studies of the boundary-layer flow phenomena of the turbine stator blade rows are analyzed and compared.

In reference 1 the blade boundary-layer losses are described in terms of basic parameters that may be calculated from the measured total-pressure losses in the blade wakes. The results of an experimental mean-radius flow survey taken a few thousandths of an inch downstream of the trailing edges of a set of transonic turbine stator blades are presented in terms of the fundamental boundary-layer parameters in reference 2. A method for theoretically calculating the boundary-layer thickness from turbulent-boundary-layer theory is also presented in the reference. The experimental and theoretical data are in reasonable agreement. The results of an experimental annular flow survey about 1/4 inch downstream of the trailing edges of similar blades are presented in reference 3. A method is given for calculating the total stator loss for known mean-radius losses.

In the current investigation, experimental flow surveys similar to those described in references 2 and 3 have been made for the stator used in the two high subsonic Mach number turbines of references 4 and 5. Theoretical calculations for the turbulent-boundary-layer thickness have also been made using the method of reference 2. The method of reference 3 is used to calculate the three-dimensional stator loss from mean-radius flow surveys. The results of these experimental and theoretical stator blade-outlet boundary-layer studies are presented and compared herein.

## SYMBOLS

$\mathscr{A}$ aspect ratio based on mean-section chord

$a'_{cr}$ critical velocity of sound, $\sqrt{\frac{2\gamma}{\gamma + 1} gRT'}$, ft/sec

c mean-section chord length, ft

E energy factor, $\psi/\theta$ or $\psi^*/\theta^*$

g acceleration due to gravity, 32.17 ft/sec$^2$

H form factor, $\delta/\theta$ or $\delta^*/\theta^*$

n exponent used in describing boundary-layer velocity profile

P pressure factor, $\xi/\theta$ or $\xi^*/\theta^*$

p pressure, lb/sq in.

R gas constant, 53.35 ft-lb/(lb)($^\circ$R)

| | |
|---|---|
| $r$ | radius, in. |
| $s$ | mean-section blade spacing, ft |
| $T'$ | total temperature, $^{o}R$ |
| $V$ | gas velocity, ft/sec |
| $\alpha_s$ | mean-section stagger angle measured from axial direction, deg |
| $\beta$ | blade-outlet flow angle measured from axial direction, deg |
| $\gamma$ | ratio of specific heats |
| $\delta$ | boundary-layer displacement thickness, ft |
| $\delta^*$ | displacement-thickness parameter, $\delta/(s \cos \beta)$ |
| $\theta$ | boundary-layer momentum thickness, ft |
| $\theta^*$ | momentum-thickness parameter, $\theta/(s \cos \beta)$ |
| $\xi$ | boundary-layer pressure thickness, ft |
| $\xi^*$ | pressure-thickness parameter, $\xi/(s \cos \beta)$ |
| $\sigma$ | mean-section solidity |
| $\psi$ | boundary-layer energy thickness, ft |
| $\psi^*$ | energy-thickness parameter, $\psi/(s \cos \beta)$ |

Subscripts:

| | |
|---|---|
| fs | free stream |
| m | mean |
| meas | measured |
| p | pressure surface |
| s | suction surface |
| t | tip |
| tot | sum of suction- and pressure-surface quantities |

0 station about 1 in. upstream of stator leading edge

1 station immediately downstream of stator trailing edge where mean-radius surveys were made

1a station about 1/4 in. downstream of stator trailing edge where annular surveys were made

2 station representing blade exit conditions after mixing

3-D three-dimensional

Superscript:

' total state

## DESCRIPTION OF STATOR AND EXPERIMENTAL PROCEDURE

A detailed description of the stator blades and the method used in their design is given in reference 4. The stator was designed for free-vortex flow at the exit with a design exit critical velocity ratio at the mean section of about 0.91. The blade suction surface downstream of the throat is straight. There is a considerable amount of taper in the axial chord of the blade, varying from 0.69 inch at the hub section to 1.79 inches at the tip (fig. 1). Thirty blades were used, having values of solidity of 1.3, 1.5, and 1.6 for the hub, mean, and tip sections, respectively.

The experimental data were obtained from both mean-radius and annular surveys. The annular surveys were taken while the turbine was running at rotor blade speed corresponding approximately to the point of maximum over-all efficiency at each pressure ratio. The instrumentation for the mean-radius surveys required that the rotor be removed for these tests. For all the tests, the absolute inlet total pressure was maintained at about 50 inches of mercury (24.6 lb/sq in. abs) and the temperature was about 70° F. All traverse-probe measurements for both the mean-radius and annular surveys were transmitted to a recorder and plotted against the circumferential distance traversed by the probe. The free-stream total conditions at the survey stations were determined by four total-pressure probes and four thermocouples located upstream in the plenum chamber. The stator-inlet static pressure was measured by averaging the readings from 12 taps, six on the inner and six on the outer wall of the annulus about 1 inch upstream of the stator leading edge (station 0, fig. 1(b)). Using the measured values of inlet static pressure, inlet total temperature, weight flow, and annulus area, the stator-inlet total pressure $p_0'$ was calculated from equation (4) of reference 4. The inner- and

outer-shroud static pressures at the blade exit were measured by 18 taps, 15 located in the inner shroud and three located in the outer shroud, all about 1/4 inch downstream of the blade trailing edge (station 1a).

The mean-radius surveys consisted of circumferential traverses across 1/2 blade spacing (including one complete blade wake) with a total-pressure probe that was alined with the flow angle. The probe was a single-tube hook type with a sensing element 0.015 inch wide. It was adjusted to only a few thousandths of an inch axial clearance with the blade trailing edge (station 1). Twenty-one surveys were made over a range of blade-exit critical velocity ratio $(V/a'_{cr})_{fs,m,1}$ from approximately 0.5 to 1.1 by adjusting the blade-exit static pressure.

The annular surveys consisted of circumferential traverses across approximately $1\frac{1}{2}$ blade spacings at each of 24 radial stations about 1/4 inch downstream from the stator blade trailing edge (station 1a). The distance between radial stations in the regions near the hub and tip was less than that for the remainder of the blade because of the greater variation of losses in those regions. Total-pressure and flow-angle measurements were made with a cobra-type probe. A wedge-type probe was used to measure static pressure. Photographs of similar probes are shown in figure 2 of reference 6. The annular surveys were made at values of mean-radius blade-exit critical velocity ratio $(V/a'_{cr})_{fs,m,1}$ of 0.630, 0.757, 0.837, and 1.083.

Where the flow velocities were supersonic, no correction was made for the normal-shock loss of a detached bow wave ahead of the probe. The observed loss in total pressure for this condition of operation was probably caused by oblique shock waves in the blade passage and at the trailing edge in addition to a weakend normal-shock loss ahead of the probe, as discussed in reference 2. Thus, the application of a normal-shock-loss correction based on the isentropic free-stream velocity would overcompensate for this loss. The results obtained with supersonic flow velocities are therefore subject to error.

## THEORETICAL CALCULATIONS AND ANALYSIS OF DATA

Two separate analyses of the stator survey data are considered herein. First, the results of the mean-radius survey of the blade wake just downstream of the trailing edges (station 1) are compared with a theoretical calculation of the boundary-layer momentum thickness. Secondly, the over-all stator total-pressure ratio as determined by the complete annular surveys at station 1a is compared with calculated values based on the mean-radius surveys at station 1.

## Comparison of Measured Boundary-Layer Characteristics with Theoretical Results

Several of the blade-outlet total-pressure traces over a range of pressure ratios are presented in figure 2. These traces were analyzed in the same manner as described in reference 2. The blade over-all boundary-layer parameters $\delta^*_{tot}$, $\theta^*_{tot}$, $\xi^*_{tot}$, and $\psi^*_{tot}$ were obtained by integrating the velocity, mass flow, and total pressure along a circumferential path across one blade pitch using equations (17) of reference 1. The free-stream total pressure was assumed over the portions of the circumferential distance not covered in the surveys. Figure 2(f) shows the relations among various momentum-thickness parameters. The relations among the other thickness parameters are similar. The parameters $H_{tot}$, $P_{tot}$, and $E_{tot}$ were obtained from these calculated parameters.

The theoretical boundary-layer momentum thickness from turbulent-boundary-layer theory was calculated using equation (6) of reference 2 for values of free-stream mean-radius blade-outlet critical velocity ratio $(V/a'_{cr})_{fs,m,1}$ of 0.512, 0.602, 0.691, 0.782, and 0.915. The blade surface velocity distributions for these five points were calculated by a three-dimensional design method (ref. 4) and are shown in figure 3.

## Use of Mean-Radius Boundary-Layer Parameters in Predicting Three-Dimensional Turbine Stator Losses and Comparison with Values Obtained from Annular Surveys

The method of reference 3 was used to calculate three-dimensional stator losses from the results of the experimental surveys at the blade trailing edge at the mean radius. This method assumes that the average momentum loss on the blade surfaces as well as that on the inner and outer stator walls is represented by an effective momentum thickness occurring at the blade mean section. With this assumption, the following relation was developed (eq. (4), ref. 3):

$$\theta^*_{1,3\text{-}D} = \left(1 + \frac{\cos \alpha_s}{\sigma \mathscr{A}}\right)\left(\frac{\theta_{tot}}{c}\right)_{m,1} \frac{\sigma}{\cos \beta_{m,1}}$$

With this relation, along with those given by equations (5) and (6) of reference 3 and equation (C22) of reference 1, the over-all three-dimensional loss total-pressure ratio $p'_2/p'_0$ can be calculated.

The method used herein for calculating the boundary-layer parameters and over-all loss total-pressure ratio $p_2'/p_0'$ from the annular surveys at station 1a is also identical to that given in reference 3.

For the test facility used in the subject investigation, the value of the ratio of calculated inlet total pressure to free-stream total pressure as measured in the plenum chamber $p_0'/p_{fs,meas}'$ varied from 0.999 to 0.997 over the range of exit velocities investigated.

## RESULTS AND DISCUSSION

As in the previous section, the two analyses are considered separately. The results of the theoretical calculation of the turbulent boundary-layer thickness are first compared with the experimental data from the mean-radius trailing-edge surveys. The results obtained from the annular surveys of the stator are also presented. The over-all total-pressure ratio obtained from the annular surveys is compared with that calculated from the mean-radius survey in the plane of the blade trailing edge.

### Comparison of Measured Boundary-Layer Characteristics with Theoretical Results

Over-all form and loss factors. - The three boundary-layer factors $H_{tot}$, $E_{tot}$, and $P_{tot}$ were evaluated for each of the mean-radius trailing-edge surveys, and are shown as a function of the free-stream critical velocity ratio $(V/a_{cr}')_{fs,m,1}$ in figure 4. The experimental values of all three parameters agree closely with the theoretical curves for a simple-power-law velocity profile evaluated by equations (B12) to (B14) of reference 1, using an exponent $n$ of $1/7$.

Blade surface boundary-layer momentum thickness. - The experimentally obtained momentum-thickness-to-chord ratios for the blade pressure and suction surfaces as well as the over-all or total value are compared with the theoretically calculated values over a range of exit free-stream critical velocity ratio in figure 5. Although there is some scatter in the experimentally obtained points, there is a slight trend toward decreased momentum-thickness ratio with increasing exit velocity.

Good agreement is obtained between the measured and theoretical values of boundary-layer momentum thickness at the relatively low values of the blade-outlet free-stream critical velocity ratio of 0.50 to 0.60. However, at higher velocities the measured values, particularly on the blade suction surface, are somewhat higher than those calculated theoretically. This is probably due in large part to secondary flow of the low-momentum fluid in the boundary layer. Apparently, a considerable portion of the boundary-layer fluid developed on the outer annulus wall and on the blade surface at radii above the blade mean radius flows radially inward and is measured as it flows off the blade at the mean radius. Visual evidence of such radial inflow of the low-momentum boundary layer along the blade suction surface, particularly at high Mach number levels, is presented in reference 7.

## Results of Annular Surveys and Comparison with Over-All Stator Loss Calculated from Mean-Radius Surveys

The ratios of the measured total pressure $p'_{la}/p'_{fs,meas}$ are plotted as contours in figure 6 for four values of blade-outlet critical velocity ratio $(V/a'_{cr})_{fs,m,1}$. There is a marked change in the distribution of losses with increasing velocity. The area of the loss region along the outer annulus wall is nearly constant, while the total-pressure losses in the blade wake and in the area near the hub increase considerably with increasing exit velocity. These results support the premise that there is a radial inflow of low-momentum boundary-layer fluid and that the amount of radial inflow increases with increasing velocity level. This effect would explain in part the result obtained in the previous section where the measured value of momentum loss at the mean radius at the higher velocity levels was greater than the theoretical value based on two-dimensional theoretical analysis of the turbulent boundary layer.

For the three annular surveys at subsonic exit velocities, the radial variation of the static pressure was determined from the wall static-pressure taps and average readings of the exit static pressure obtained from the circumferential surveys at each radius. For the high-velocity survey, for which $(V/a'_{cr})_{fs,m,1}$ was equal to 1.083, a linear variation between the hub and tip wall static-pressure tap readings was assumed. The radial variation of velocity corresponding to these static pressures and the free-stream total pressure is presented in figure 7 for the four annular surveys.

The radial variations of the boundary-layer parameters $\theta^*_{1a}$ and $\delta^*_{1a}$ for the four annular surveys are shown in figure 8. The hub losses are again shown to be considerably higher than those occurring at the tip and increase with the higher exit velocities.

The over-all loss total-pressure ratio as determined from the annular surveys is compared in figure 9 with that calculated from the mean-radius boundary-layer characteristics measured at station 1. The values of loss total-pressure ratio as computed from the four annular surveys are all somewhat higher than the values computed from mean-radius surveys. It is likely that radial inward flow of the low-momentum fluid near the blade tip caused the loss measured at the mean radius to be greater than an average value for the whole blade passage.

## SUMMARY OF RESULTS

Theoretical and experimental studies of the boundary-layer flow for a turbine stator over a range of velocities have been made. The following results were obtained:

1. The values of the boundary-layer form and loss factors, $H_{tot}$, $E_{tot}$, and $P_{tot}$, calculated from mean-radius trailing-edge surveys agree closely with theoretical values for a simple-power-law velocity profile having an exponent of 1/7.

2. For exit critical velocities of about 0.5 to 0.6, good agreement was obtained between measured values of boundary-layer momentum thickness and theoretical values calculated assuming a turbulent boundary layer on the blade surface. At the higher velocity levels, the measured values are higher than those calculated theoretically. It is probable that the higher measured values were caused by inward radial flow of low-momentum boundary-layer fluids from the outer portion of the blade.

3. The annular surveys to obtain total-pressure contours downstream of the stator indicate that the losses measured near the hub of the stator are considerably greater than those near the tip section. This effect, which increases at higher velocity levels, may also be due to the radial inflow of low-momentum fluids along the blade surfaces as well as in the wake region downstream of the blade trailing edges.

4. The over-all total-pressure ratio across the stator was calculated both from the annular-survey results and from the mean-radius-survey results assuming that the measured boundary-layer momentum loss at the mean section could be used as the average for the whole blade passage. The values of over-all total-pressure ratio as calculated from the annular-survey results are somewhat higher than the values calculated from the

mean-radius-survey results over the range of stator-outlet velocities investigated. Apparently, radial inward flow of the low-momentum fluid near the blade tip caused the loss measured at the mean section to be greater than an average value for the whole blade passage.

Lewis Flight Propulsion Laboratory
National Advisory Committee for Aeronautics
Cleveland, Ohio, November 28, 1956

## REFERENCES

1. Stewart, Warner L.: Analysis of Two-Dimensional Compressible-Flow Loss Characteristics Downstream of Turbomachine Blade Rows in Terms of Basic Boundary-Layer Characteristics. NACA TN 3515, 1955.

2. Whitney, Warren J., Stewart, Warner L., and Miser, James W.: Experimental Investigation of Turbine Stator-Blade-Outlet Boundary-Layer Characteristics and a Comparison with Theoretical Results. NACA RM E55K24, 1956.

3. Stewart, Warner L., Whitney, Warren J., and Wong, Robert Y.: Use of Mean-Section Boundary-Layer Parameters in Predicting Three-Dimensional Turbine Stator Losses. NACA RM E55L12a, 1956.

4. Hauser, Cavour H., and Nusbaum, William J.: Experimental Investigation of a High Subsonic Mach Number Turbine Having Low Rotor Suction-Surface Diffusion. NACA RM E56G25, 1956.

5. Nusbaum, William J., and Hauser, Cavour H.: Experimental Investigation of a High Subsonic Mach Number Turbine Having High Rotor Blade Suction-Surface Diffusion. NACA RM E56I18, 1956.

6. Petrash, Donald A., Schum, Harold J., and Davison, Elmer H.: Component Performance Investigation of J71 Experimental Turbine. VIII - Effect of First-Stator Adjustment; Internal Flow Conditions of J71-97 Turbine with 70-Percent-Design Stator Area. NACA RM E56I13, 1956.

7. Rohlik, Harold E., Kofskey, Milton G., Allen, Hubert W., and Herzig, Howard Z.: Secondary Flows and Boundary-Layer Accumulations in Turbine Nozzles. NACA Rep. 1168, 1954. (Supersedes NACA TN's 2871, 2909, and 2989.)

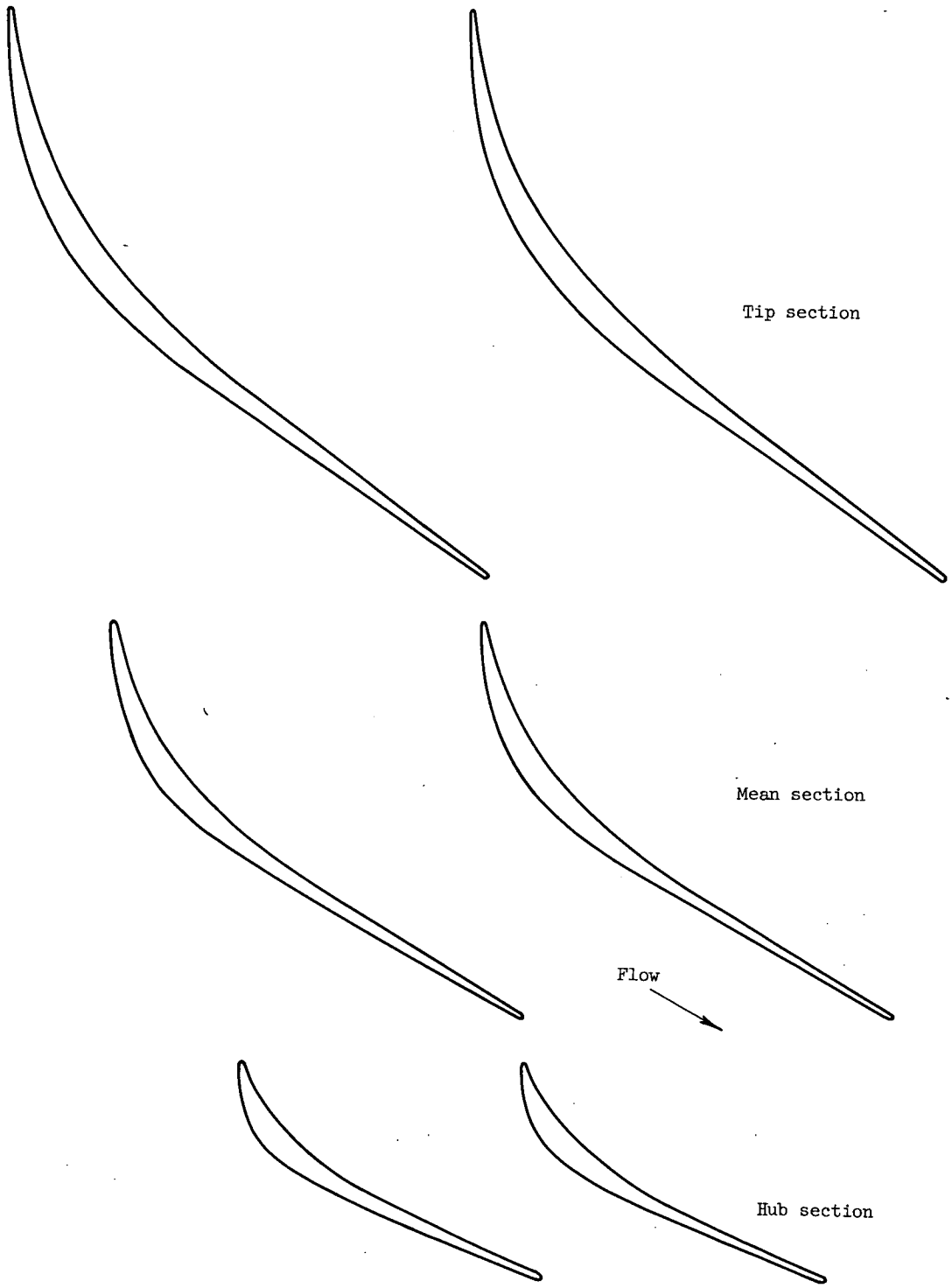


(a) Stator blade passages and profiles.

Figure 1. - Stator blade passages and profiles and a sketch of station nomenclature.

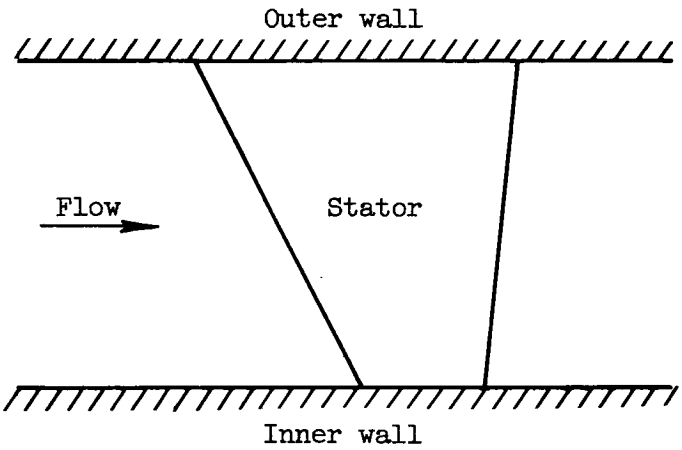


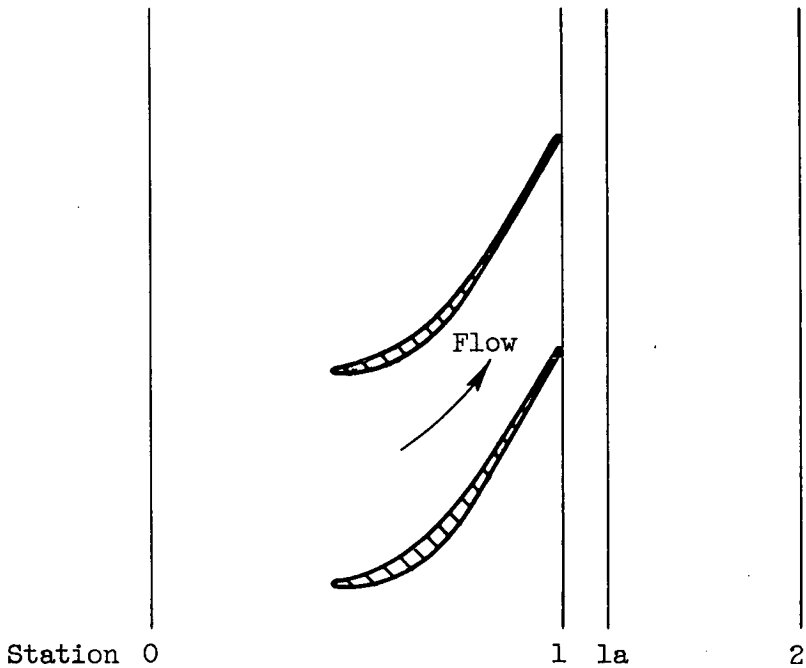


(b) Station nomenclature.

Figure 1. - Concluded. Stator blade passages and profiles and a sketch of station nomenclature.

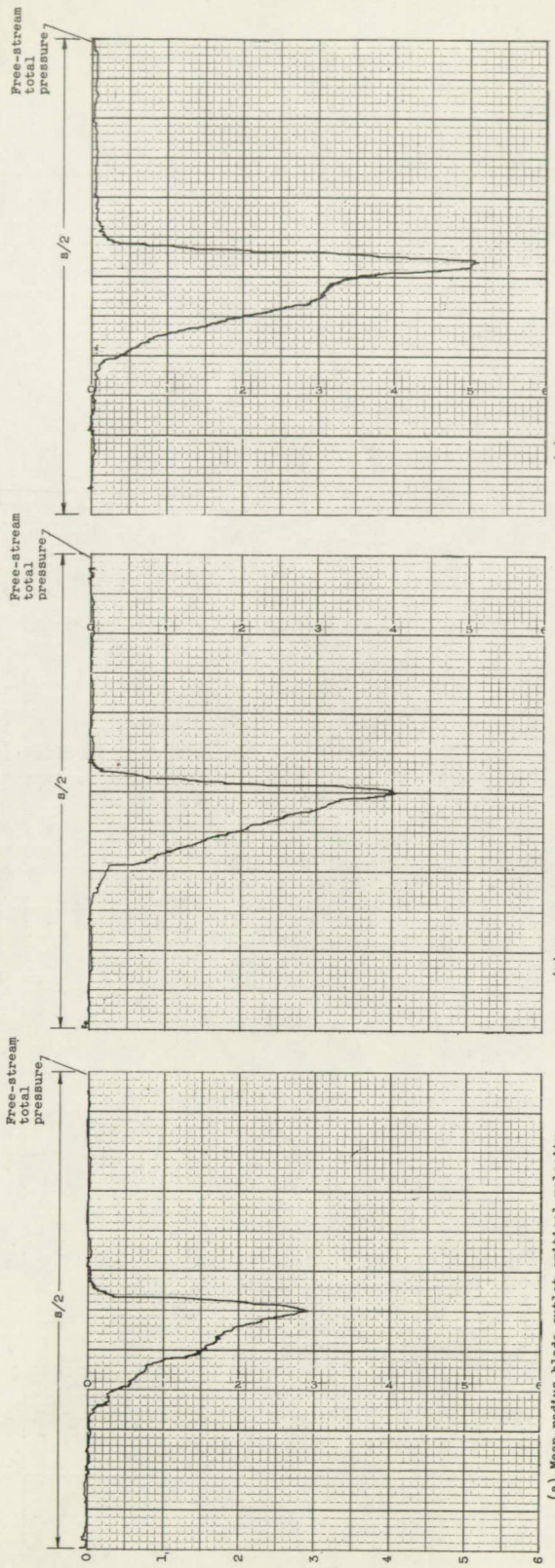


Figure 2. - Blade-outlet total-pressure traces and sketch showing relations among various momentum-thickness parameters. Free-stream total pressure, 24.37 ±0.05 pounds per square inch.

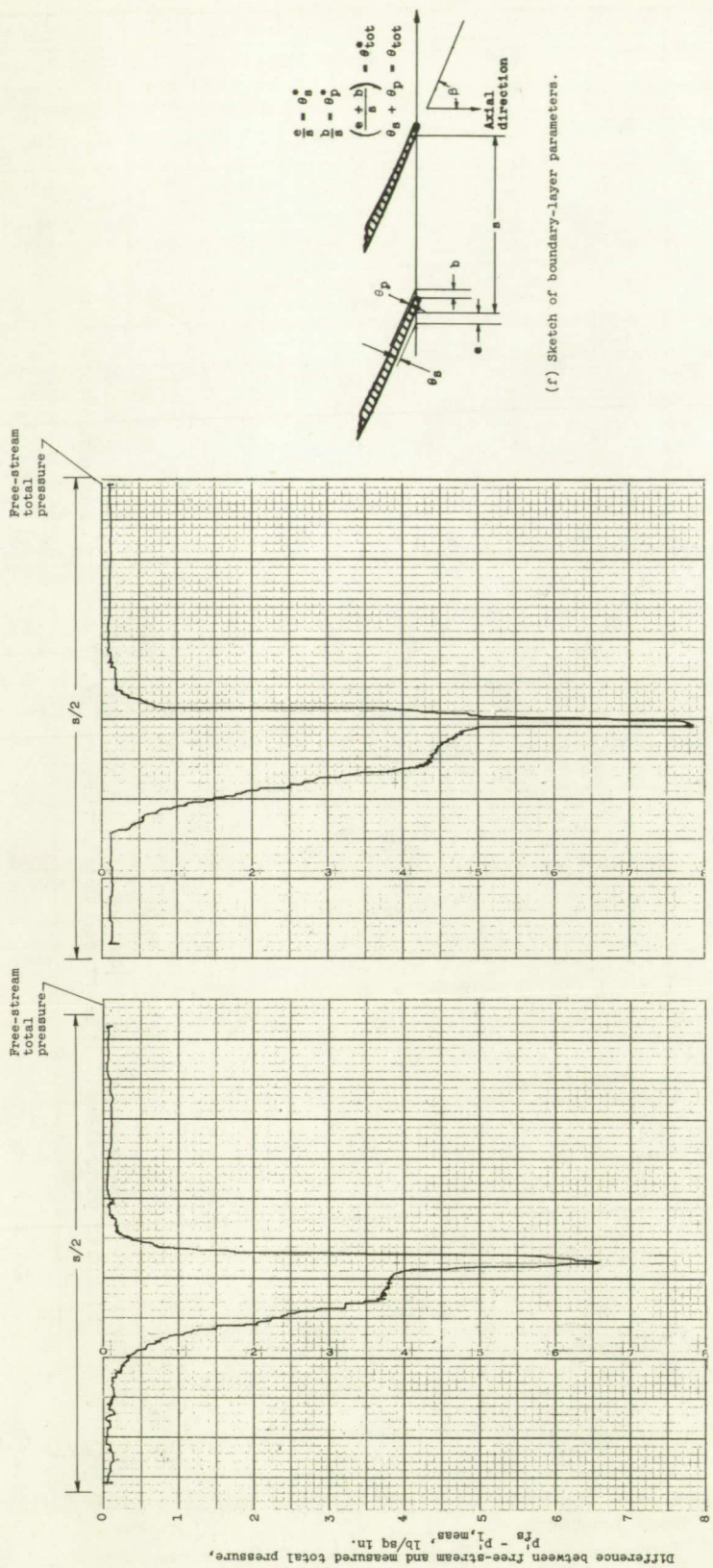


Figure 2. - Concluded. Blade-outlet total-pressure traces and sketch showing relations among various momentum-thickness parameters. Free-stream total pressure, 24.37 ±0.05 pounds per square inch.

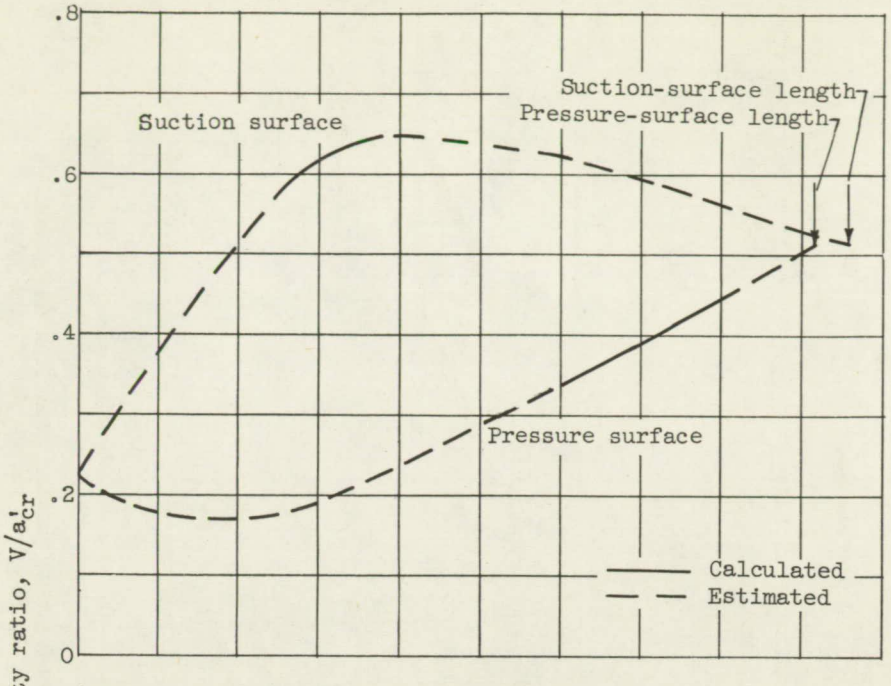


(a) Blade-outlet critical velocity ratio $(V/a'_{cr})_{fs,m,1}$, 0.512.

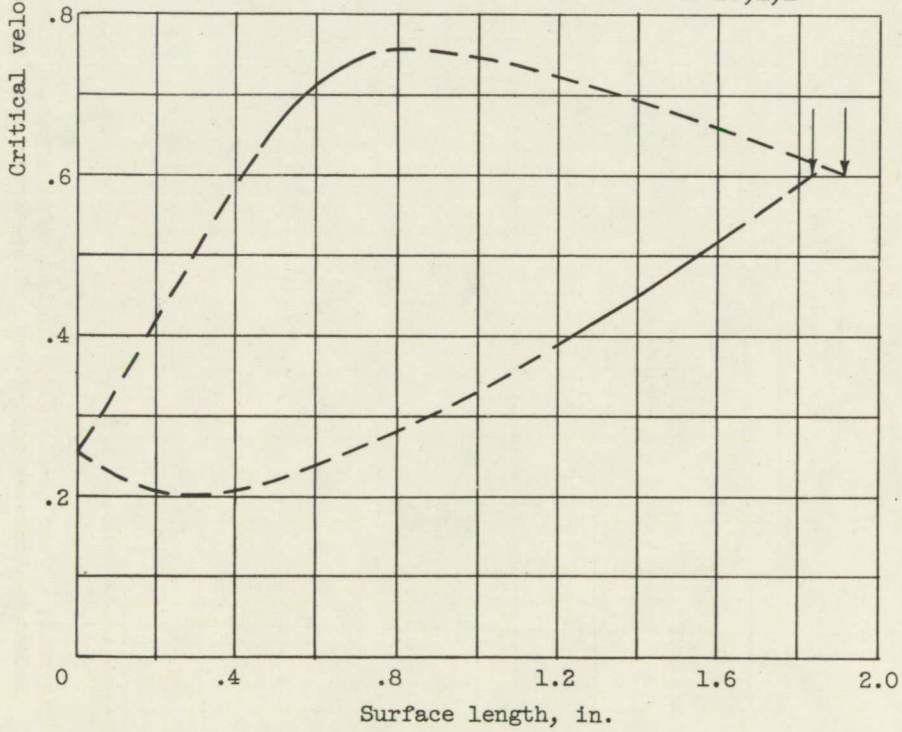


(b) Blade-outlet critical velocity ratio $(V/a'_{cr})_{fs,m,1}$, 0.602.

Figure 3. - Theoretical blade surface velocity distributions at mean section.

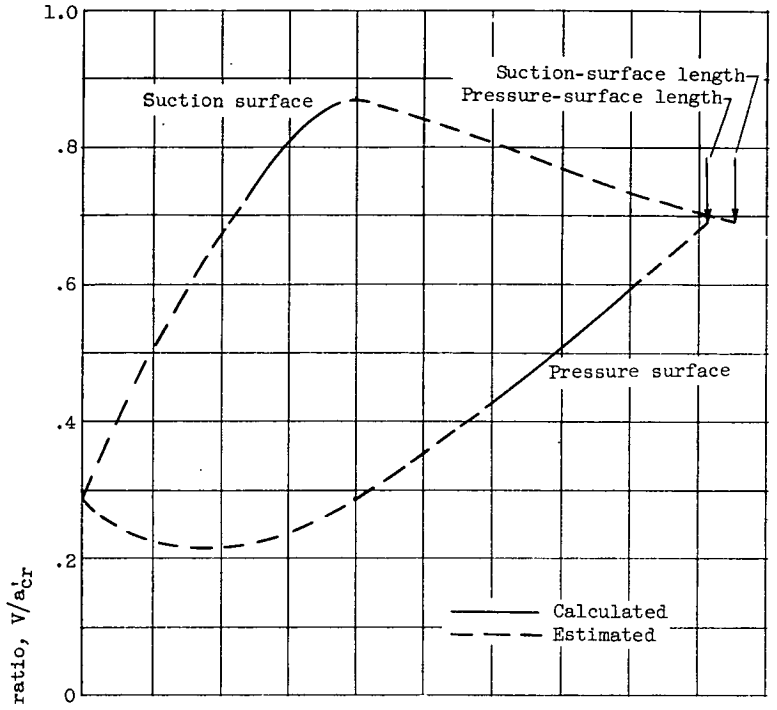


(c) Blade-outlet critical velocity ratio $(V/a'_{cr})_{fs,m,1}$, 0.691.

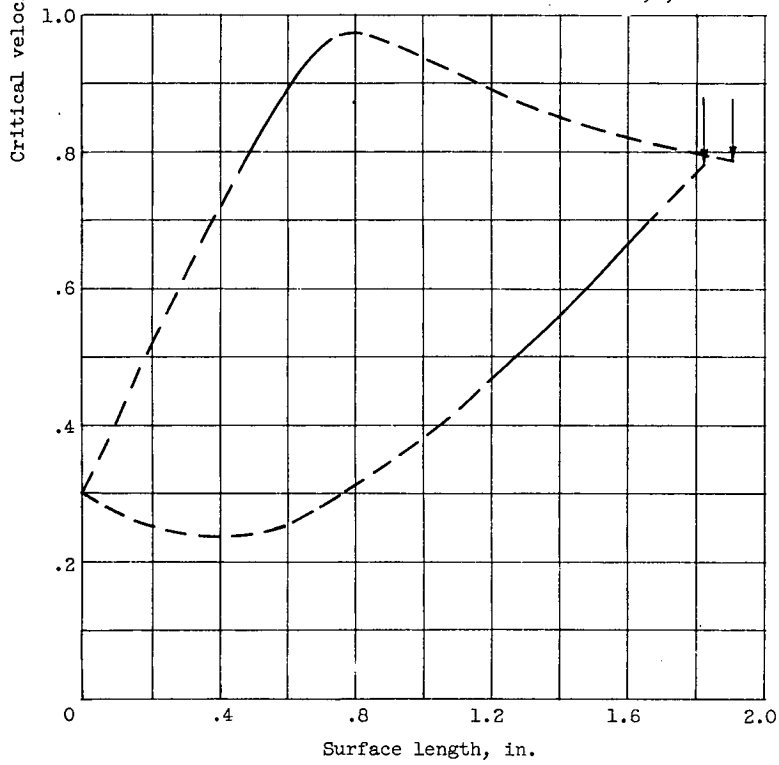


(d) Blade-outlet critical velocity ratio $(V/a'_{cr})_{fs,m,1}$, 0.782.

Figure 3. - Continued. Theoretical blade surface velocity distributions at mean section.

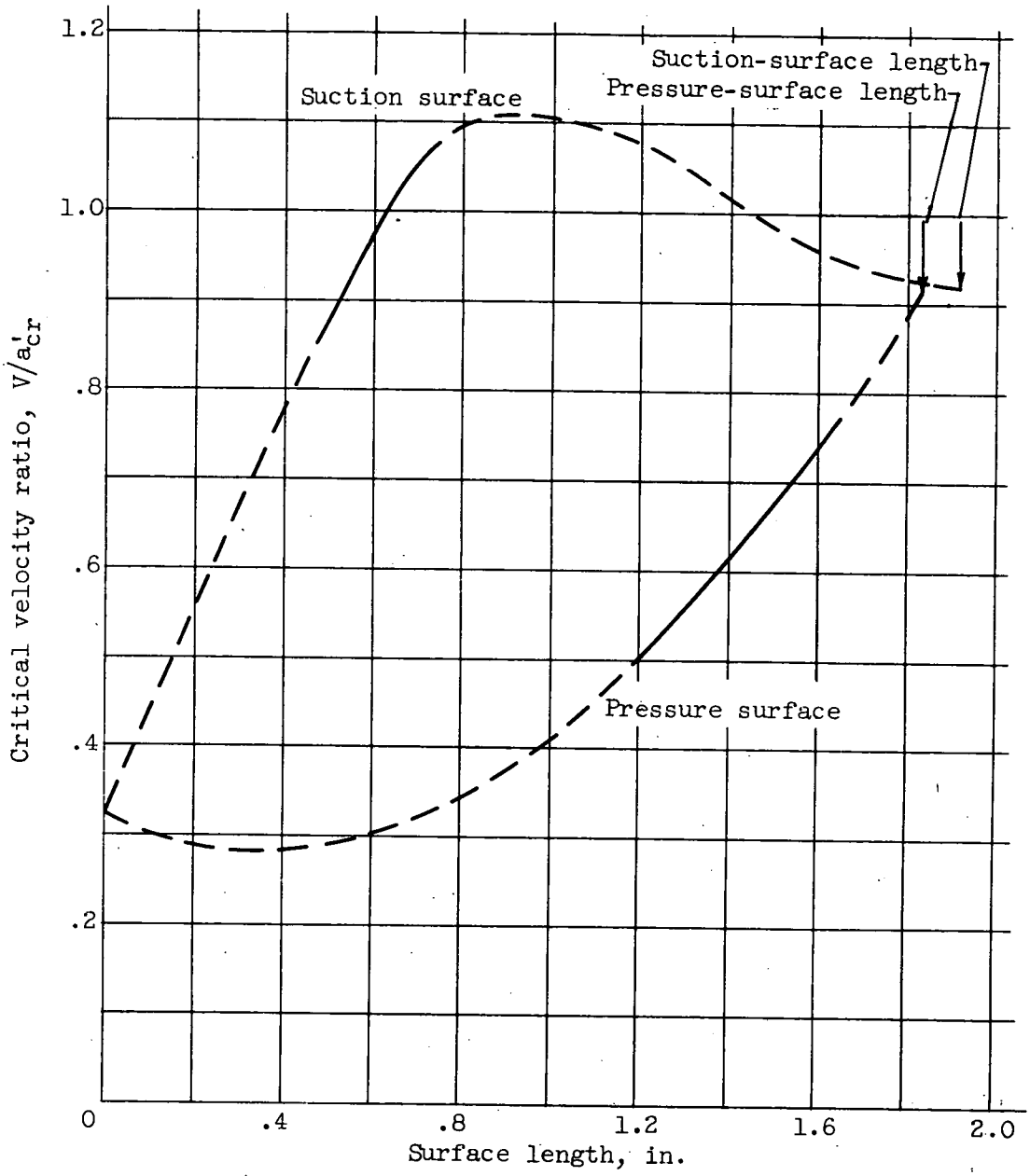


(e) Blade-outlet critical velocity ratio $(V/a'_{cr})_{fs,m,1}$, 0.915.

Figure 3. - Concluded. Theoretical blade surface velocity distributions at mean section.

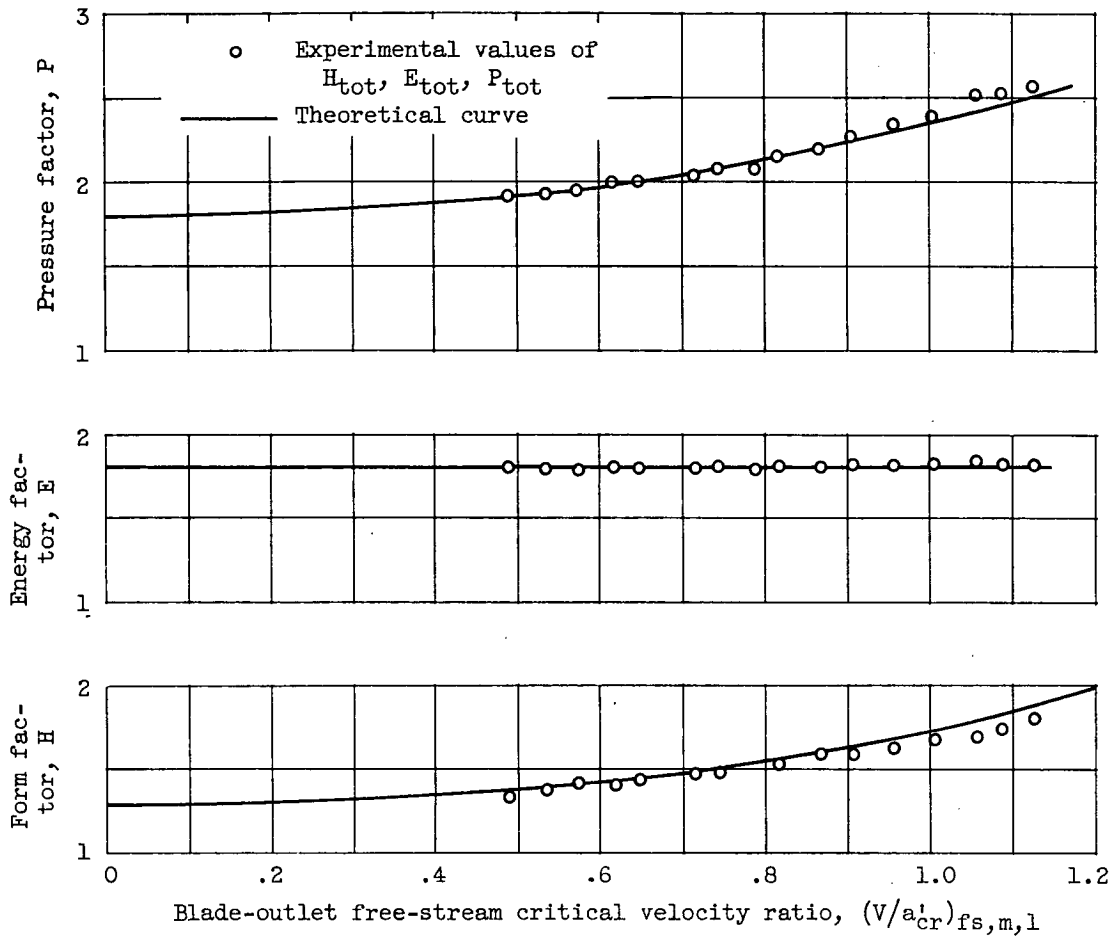


Figure 4. - Variation of boundary-layer factors with blade-outlet free-stream critical velocity ratio. Simple-velocity-profile exponent for theoretical curves, 1/7.

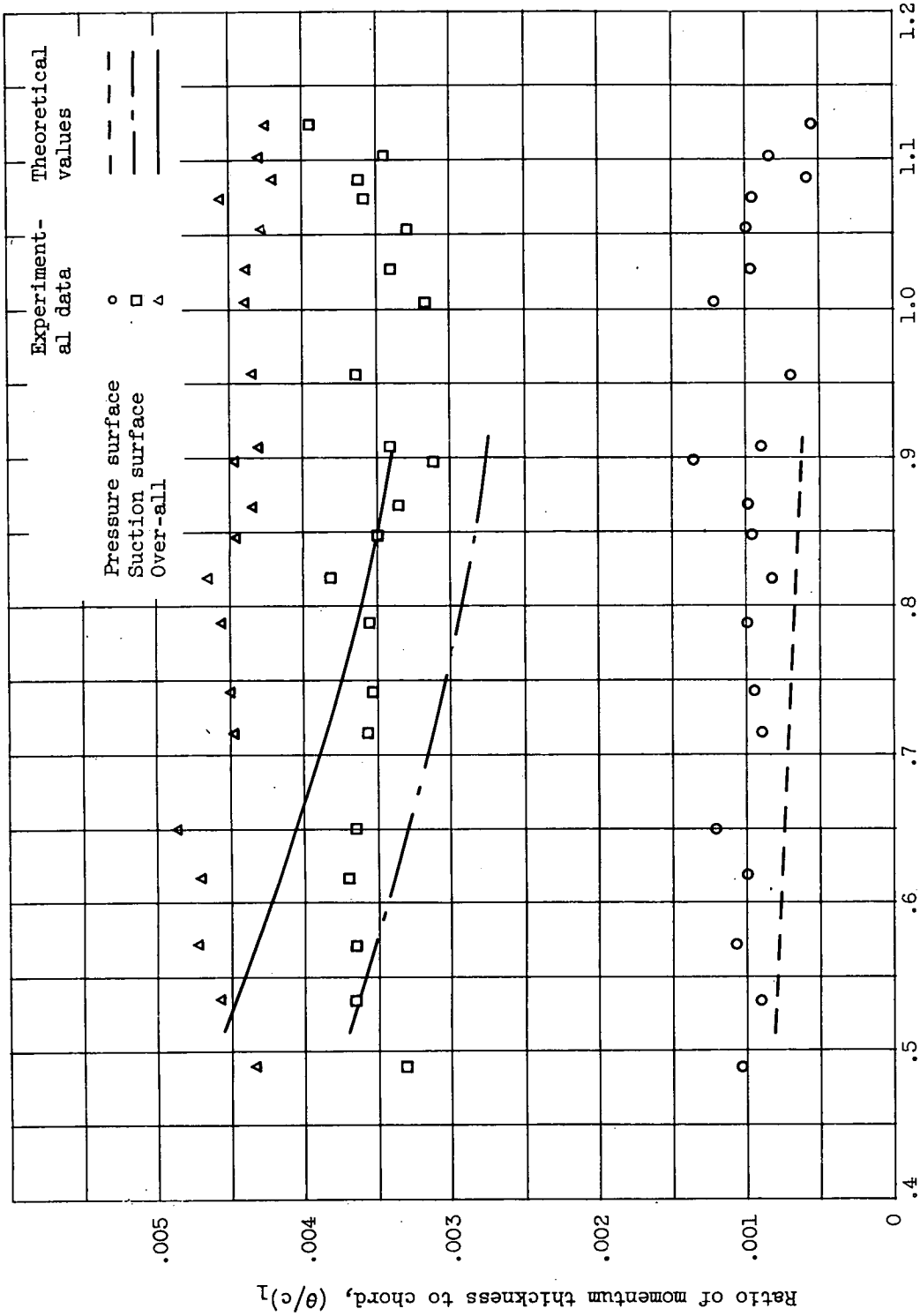


Figure 5. - Comparison of theoretical and experimental boundary-layer momentum thickness.

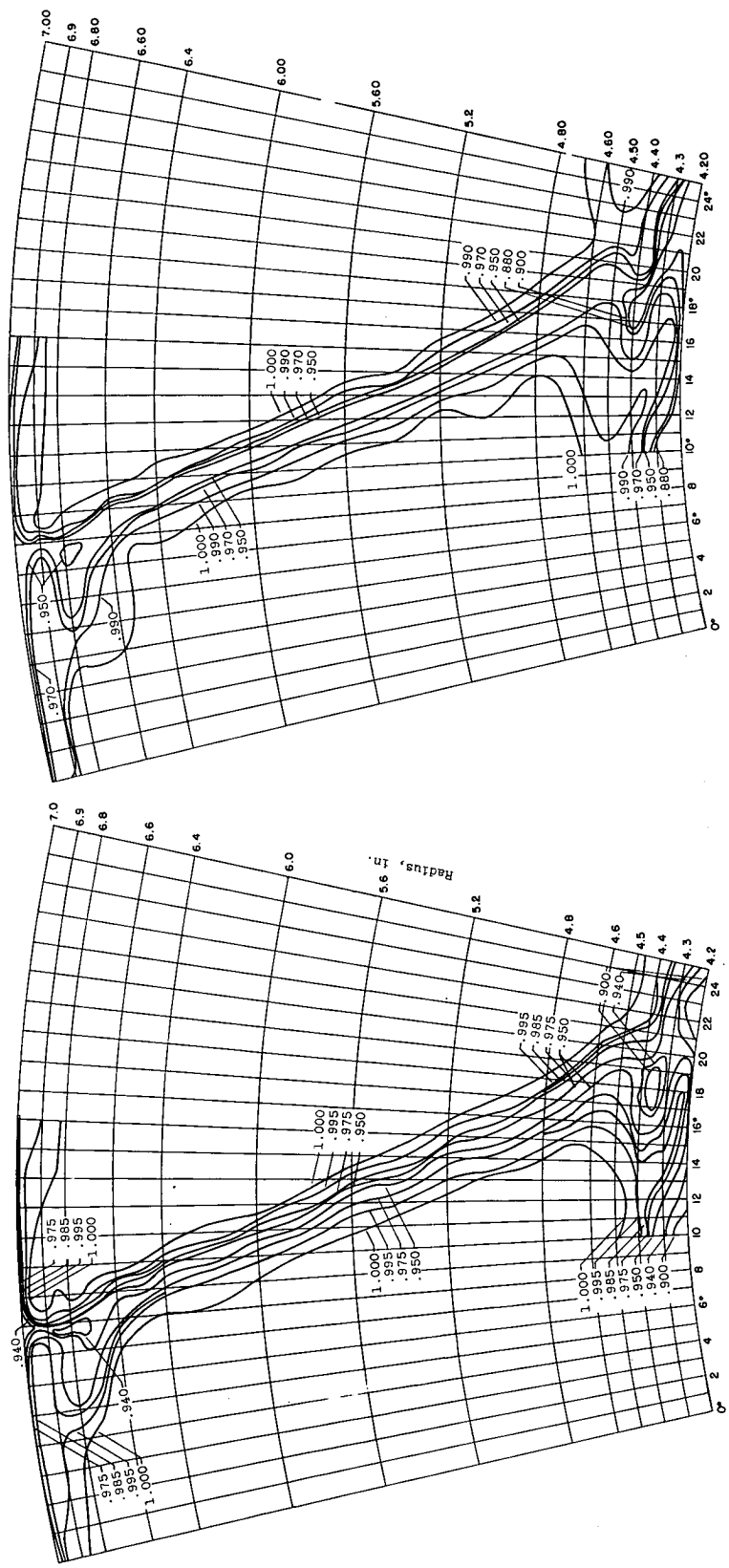


Figure 6. - Contours of total-pressure ratio $p'_{1a}/p'_{rs,meas}$ from annular surveys at blade outlet. Section corresponds to $1\frac{1}{4}$ blade passages.

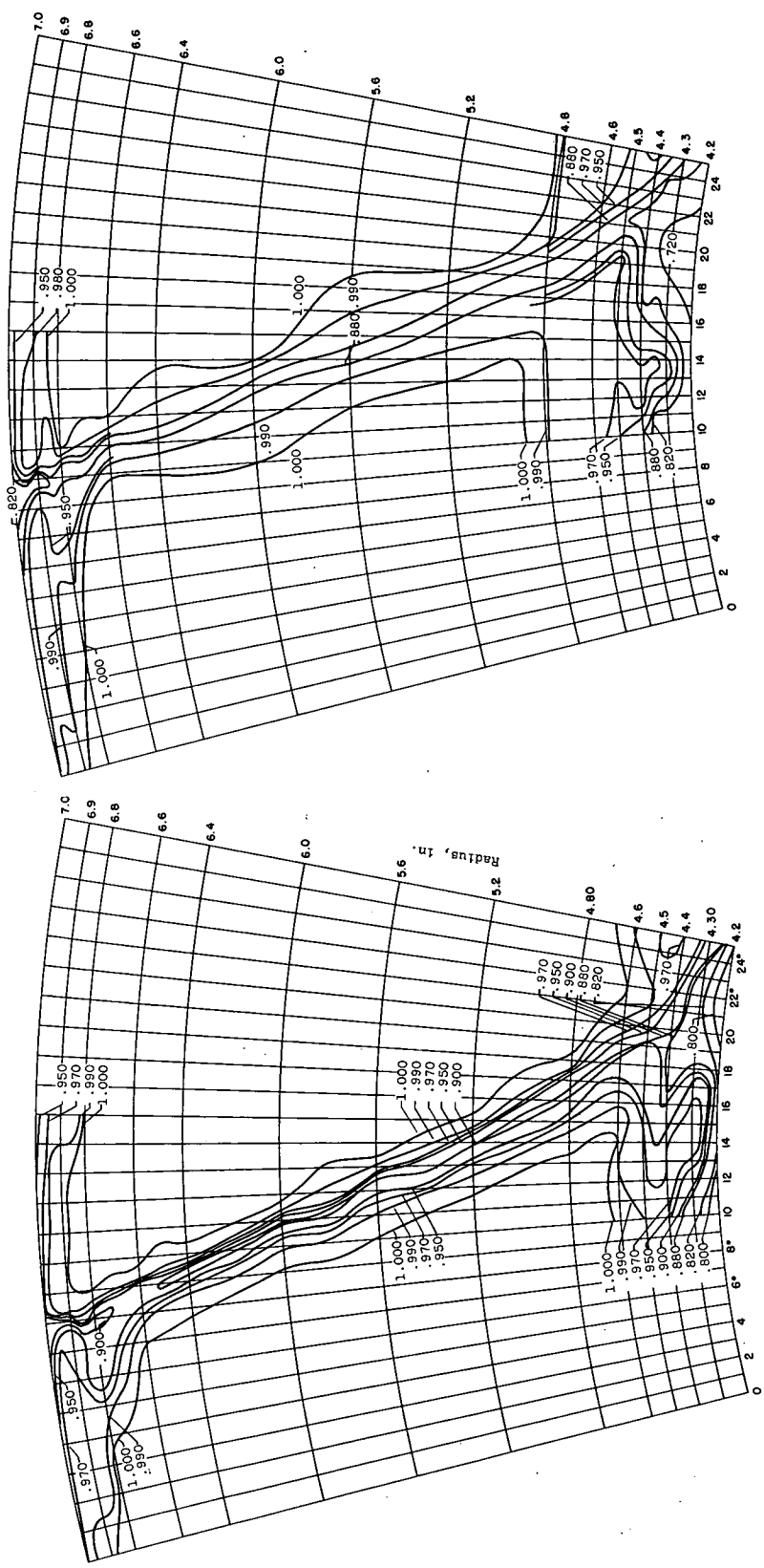


Figure 6. - Concluded. Contours of total-pressure ratio $p'_{1a}/p'_{fs,meas}$ from annular surveys at blade outlet. Section corresponds to $1\frac{1}{4}$ blade passages.

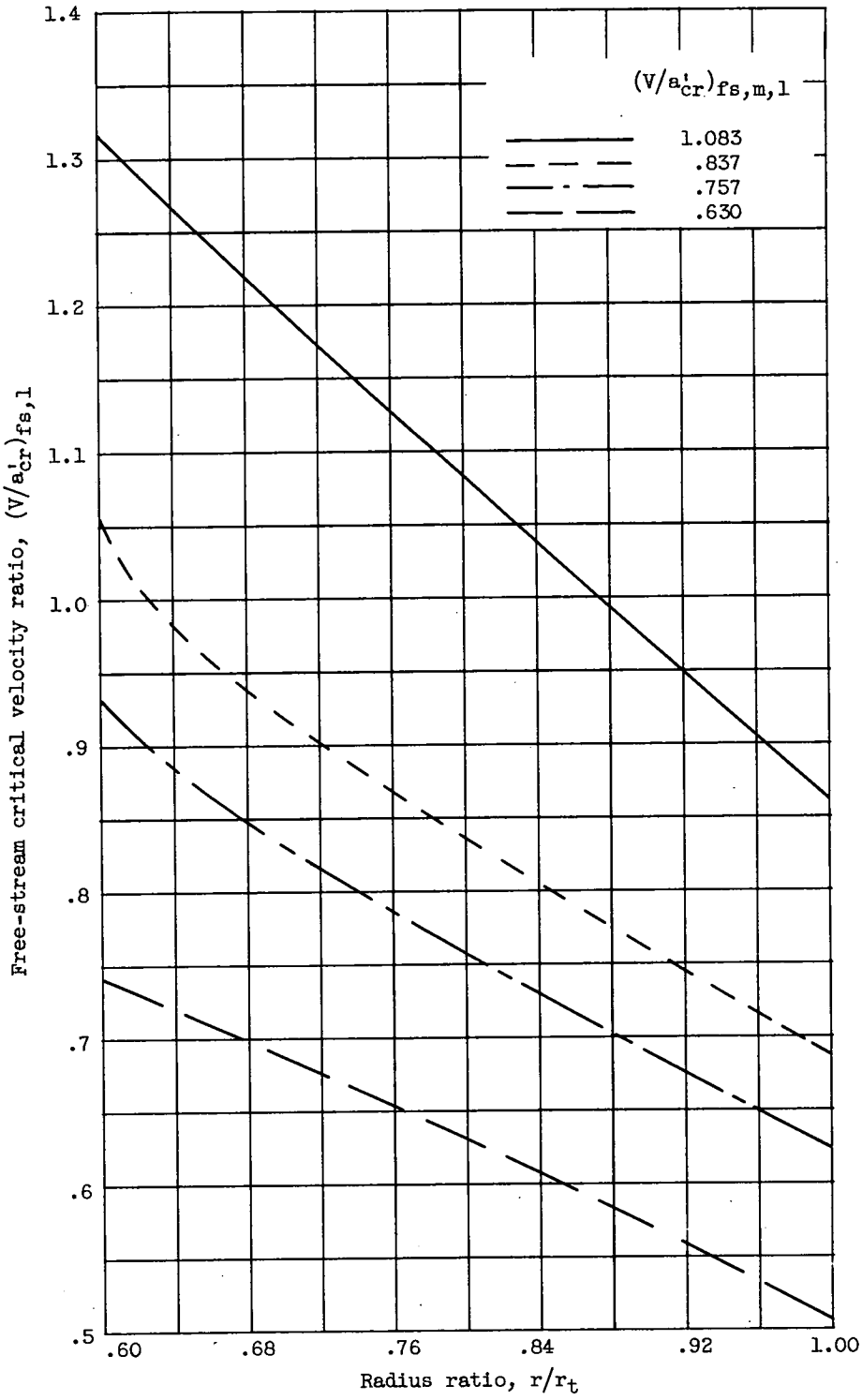


Figure 7. - Radial variation in free-stream critical velocity ratio based on results of four annular surveys.

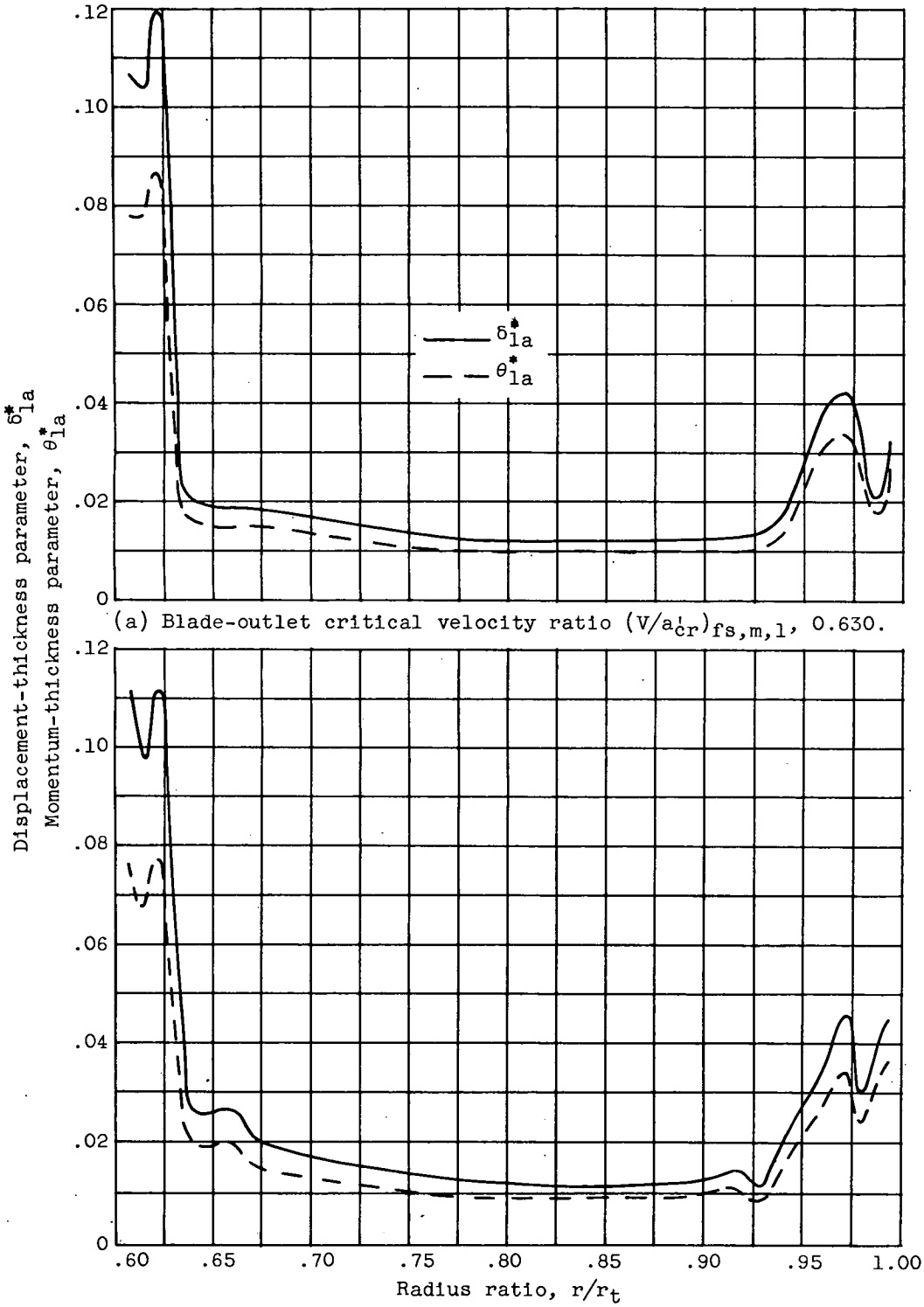


(a) Blade-outlet critical velocity ratio $(V/a'_{cr})_{fs,m,1}$, 0.630.

(b) Blade-outlet critical velocity ratio $(V/a'_{cr})_{fs,m,1}$, 0.757.

Figure 8. - Radial variation of displacement-thickness and momentum-thickness parameters based on annular surveys.

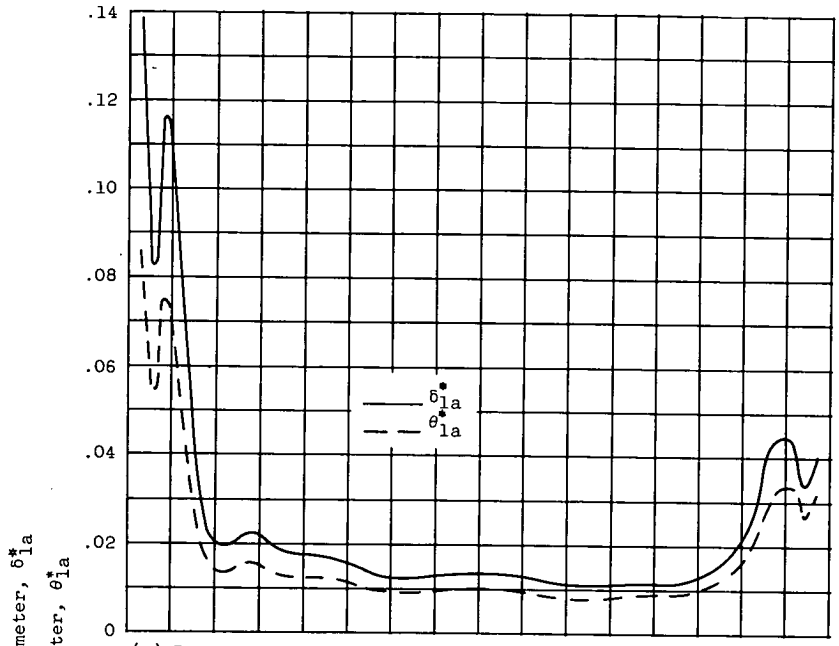


(c) Blade-outlet critical velocity ratio $(V/a'_{cr})_{fs,m,1}$, 0.837.

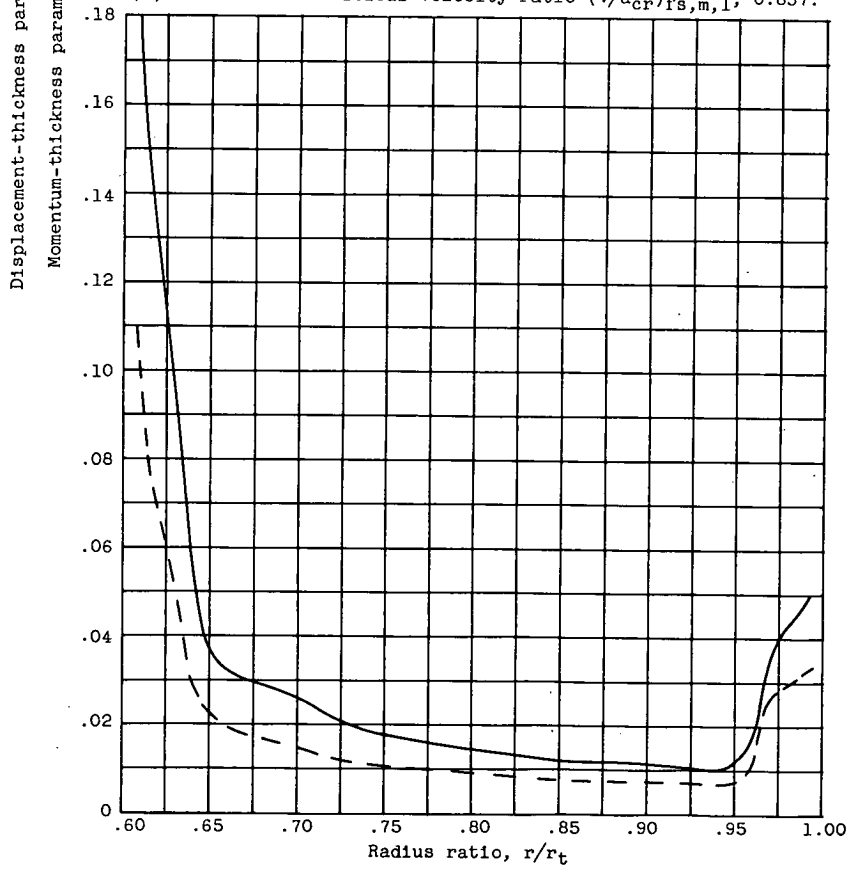


(d) Blade-outlet critical velocity ratio $(V/a'_{cr})_{fs,m,1}$, 1.083.

Figure 8. - Concluded. Radial variation of displacement-thickness and momentum-thickness parameters based on annular surveys.

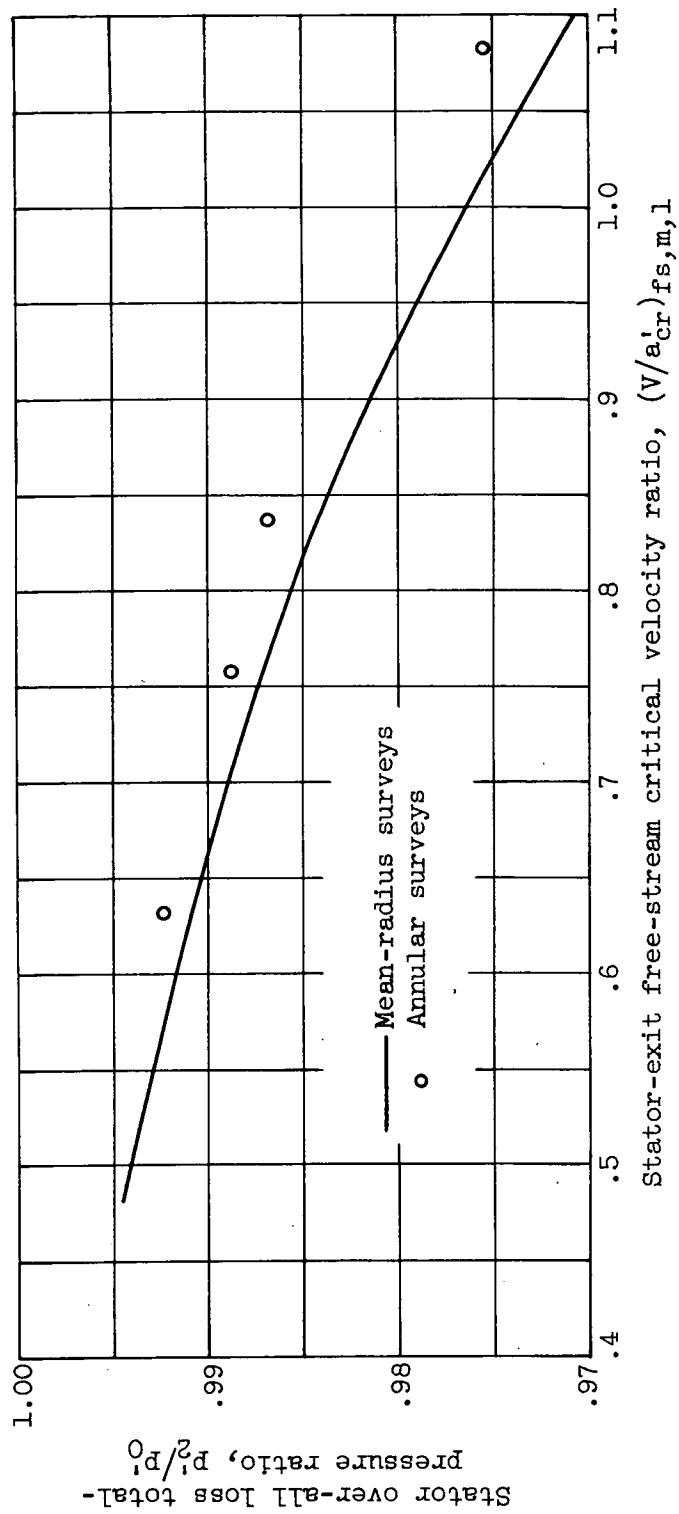


Figure 9. - Comparison of over-all loss total-pressure ratios computed from mean-radius and annular surveys.